J|A|C|S ARTICLES

Published on Web 05/20/2009

Static and Dynamic Properties of Phospholipid Bilayer Nanodiscs

Minoru Nakano,*,† Masakazu Fukuda,† Takayuki Kudo,† Masakazu Miyazaki,† Yusuke Wada,† Naoya Matsuzaki,† Hitoshi Endo,‡ and Tetsurou Handa†

Graduate School of Pharmaceutical Sciences, Kyoto University, Sakyo-ku, Kyoto 606-8501, Japan, and Institute for Solid State Physics, The University of Tokyo, 5-1-5 Kashiwanoha, Kashiwa, Chiba 277-8581, Japan

Received March 5, 2009; E-mail: mnakano@pharm.kyoto-u.ac.jp

Abstract: Nanodiscs are phospholipid−protein complexes which are relevant to nascent high-density lipoprotein and are applicable as a drug carrier and a tool to immobilize membrane proteins. We evaluated the structure and dynamics of the nanoparticles consisting of dimyristoylphosphatidylcholine (DMPC) and apolipoprotein A-I (apoA-I) with small-angle neutron scattering (SANS) and fluorescence methods and compared them with static/dynamic properties for large unilamellar vesicles. SANS revealed that the nanodisc includes a lipid bilayer with a thickness of 44 Å and a radius of 37 Å, in which each lipid occupies a smaller area than the reported molecular area of DMPC in vesicles. Fluorescence measurements suggested that DMPC possesses a lower entropy in nanodiscs than in vesicles, because apoA-I molecules, which surround the bilayer, force closer lipid packing, but allow water penetration to the acyl chain ends. Time-resolved SANS experiments revealed that nanodiscs represent a 20-fold higher lipid transfer via an entropically favorable process. The results put forward a conjunction of static/dynamic properties of nanodiscs, where the entropic constraints are responsible for the accelerated desorption of lipids.

Introduction

Phospholipid bilayer nanodiscs are lipid−protein complexes in which amphipathic helices, such as apolipoprotein A-I (apoA-I) and its truncated proteins, surround the edge of the bilayer.[1−4] They have attracted researchers' attention in recent years from a biological perspective, since apolipoprotein−lipid disclike particles are initially formed in the biogenesis of high-density lipoproteins,[5−7] and for pharmaceutical applications,[8−10] since these particles are fully biocompatible. Nanodiscs have been used as a tool to investigate the function of membrane proteins by incorporating them into the bilayer while retaining their native structure.[4,11,12]

Nanodiscs can be formed by simply mixing proteins (such as apoA-I) and lipids (such as dimyristoylphosphatidylcholine (DMPC)) at the gel−liquid crystalline phase transition temperature of the lipid or by solubilizing these compounds into a micellar solution of cholate with subsequent removal of the surfactant by dialysis or using biobeads. The reported size of nanodiscs constituted by apoA-I ranges from 7 to 12 nm, depending on the lipid/protein composition.[13−16] ApoA-I contains a series of highly homologous 11- and 22-residue amphipathic α-helices,[17,18] which are responsible for its lipid-associating properties.[17] In the nanodisc, two or more apoA-I molecules surround the hydrophobic edge of the lipid bilayer in a beltlike fashion.[19−21] However, their detailed structure and characteristics, especially the dynamic properties of lipids in

† Kyoto University.
‡ The University of Tokyo.

(1) Bayburt, T. H.; Grinkova, Y. V.; Sligar, S. G. *Nano Lett.* **2002**, *2*, 853–856.
(2) Denisov, I. G.; Grinkova, Y. V.; Lazarides, A. A.; Sligar, S. G. *J. Am. Chem. Soc.* **2004**, *126*, 3477–3487.
(3) Li, Y.; Kijac, A. Z.; Sligar, S. G.; Rienstra, C. M. *Biophys. J.* **2006**, *91*, 3819–3828.
(4) Nath, A.; Atkins, W. M.; Sligar, S. G. *Biochemistry* **2007**, *46*, 2059–2069.
(5) Duong, P. T.; Collins, H. L.; Nickel, M.; Lund-Katz, S.; Rothblat, G. H.; Phillips, M. C. *J. Lipid Res.* **2006**, *47*, 832–843.
(6) Forte, T. M.; Bielicki, J. K.; Goth-Goldstein, R.; Selmek, J.; Mccall, M. R. *J. Lipid Res.* **1995**, *36*, 148–157.
(7) Lee, J. Y.; Parks, J. S. *Curr. Opin. Lipidol.* **2005**, *16*, 19–25.
(8) Nelson, K. G.; Bishop, J. V.; Ryan, R. O.; Titus, R. *Antimicrob. Agents Chemother.* **2006**, *50*, 1238–1244.
(9) Oda, M. N.; Hargreaves, P. L.; Beckstead, J. A.; Redmond, K. A.; Van Antwerpen, R.; Ryan, R. O. *J. Lipid Res.* **2006**, *47*, 260–267.
(10) Tufteland, M.; Ren, G.; Ryan, R. O. *J. Pharm. Sci.* **2008**, *97*, 4425–4432.
(11) Bayburt, T. H.; Leitz, A. J.; Xie, G.; Oprian, D. D.; Sligar, S. G. *J. Biol. Chem.* **2007**, *282*, 14875–14881.
(12) Lyukmanova, E. N.; Shenkarev, Z. O.; Paramonov, A. S.; Sobol, A. G.; Ovchinnikova, T. V.; Chupin, V. V.; Kirpichnikov, M. P.; Blommers, M. J.; Arseniev, A. S. *J. Am. Chem. Soc.* **2008**, *130*, 2140–2141.
(13) Gianazza, E.; Eberini, I.; Sirtori, C. R.; Franceschini, G.; Calabresi, L. *Biochem. J.* **2002**, *366*, 245–253.
(14) Tricerri, M. A.; Sanchez, S. A.; Arnulphi, C.; Durbin, D. M.; Gratton, E.; Jonas, A. *J. Lipid Res.* **2002**, *43*, 187–197.
(15) Maiorano, J. N.; Jandacek, R. J.; Horace, E. M.; Davidson, W. S. *Biochemistry* **2004**, *43*, 11717–11726.
(16) Li, L.; Chen, J.; Mishra, V. K.; Kurtz, J. A.; Cao, D.; Klon, A. E.; Harvey, S. C.; Anantharamaiah, G. M.; Segrest, J. P. *J. Mol. Biol.* **2004**, *343*, 1293–1311.
(17) Segrest, J. P.; De Loof, H.; Dohlman, J. G.; Brouillette, C. G.; Anantharamaiah, G. M. *Proteins* **1990**, *8*, 103–117.
(18) Segrest, J. P.; Jones, M. K.; De Loof, H.; Brouillette, C. G.; Venkatachalapathi, Y. V.; Anantharamaiah, G. M. *J. Lipid Res.* **1992**, *33*, 141–166.
(19) Borhani, D. W.; Rogers, D. P.; Engler, J. A.; Brouillette, C. G. *Proc. Natl. Acad. Sci. U.S.A.* **1997**, *94*, 12291–12296.
(20) Martin, D. D.; Budamagunta, M. S.; Ryan, R. O.; Voss, J. C.; Oda, M. N. *J. Biol. Chem.* **2006**, *281*, 20418–20426.

 10.1021/ja9017013 CCC: $40.75

nanodiscs, are not well understood. In the present study, we elucidated the static and dynamic properties of apoA-I/DMPC nanodiscs using fluorescence and small-angle neutron scattering (SANS) techniques.

Experimental Section

ApoA-I was isolated from pig plasma using procedures described previously[22] and then denatured in a 6 M guanidine hydrochloride solution and dialyzed against Tris-buffered saline (TBS; 10 mM Tris, 150 mM NaCl, 1 mM EDTA, and 0.01 g/mL NaN_3, pH 7.4). DMPC and deuterated lipid d_{54}-DMPC were obtained from Avanti Polar Lipids, Inc. (Alabaster, AL). DMPC was mixed with TBS containing apoA-I (DMPC:apoA-I = 80:1 (mol/mol)) and incubated at 25 °C for 8 h. Nanodiscs formed were separated from coexisting vesicles and lipid-free proteins by NaBr density gradient ultracentrifugation at 40 000 rpm for 18 h in a Beckman SW50.1 rotor and dialyzed against TBS. The dispersions were condensed with Centricon YM-10 (Millipore, Bedford, MA) up to the desired concentrations. Nanodiscs consisting of either d_{54}-DMPC (D-disc) or DMPC (H-disc) were prepared. The concentration of DMPC was determined using an enzymatic assay kit for choline (Wako, Osaka, Japan).

SANS measurements were performed by the SANS-U of the Institute for Solid State Physics, The University of Tokyo, at the research reactor JRR-3, Tokai, Japan.[23] The wavelength (λ) of the neutron source was 7 Å ($\Delta\lambda/\lambda$ = 10%). The volume fraction of D_2O (ϕ_{D_2O}) and the phospholipid concentration (c_{PL}) of each preparation were adjusted using TBS prepared from H_2O and D_2O. Samples were measured in quartz cells with a pass length of 2 mm.

For structural evaluation of nanodiscs, a D-disc with $\phi_{D_2O} = 0.4$ and c_{PL} = 7.4 mM and an H-disc with $\phi_{D_2O} = 0.86$ and c_{PL} = 7.4 mM were prepared. The former provides structural information about the lipid core due to the contrast matching of the solvent and protein, while the scattering from the latter comes from the whole disc as represented in Figure 1B. The sample-to-detector distance was set at 2 and 8 m to cover a range of $0.006 \le q \le 0.15$ Å^{-1}, where q is the magnitude of the scattering vector. Scattering data measured at 37 °C were transformed to absolute cross sections using a Lupolen standard and subtracted for solvent scattering and incoherent scattering.

For time-resolved SANS (TR-SANS) experiments with nanodiscs, ϕ_{D_2O} was adjusted to 0.5, and the sample-to-detector distance was set at 4 m. After equivalent volumes of D-disc and H-disc (c_{PL} = 20.0 or 13.3 mM) were mixed, time-resolved measurement was started immediately. Scattering data were accumulated with a 2D detector to calculate the count rate (total counts/s). The count rate for the solvent was subtracted. The normalized contrast, $\Delta\rho(t)/\Delta\rho(0)$, was calculated by $\Delta\rho(t)/\Delta\rho(0) = [[I(t)]^{1/2} - [I(\infty)]^{1/2}]/[[I(0)]^{1/2} - [I(\infty)]^{1/2}]$, where $I(t)$ is the count rate at time t after LUV mixing, $I(\infty)$ is the count rate determined after a sufficiently long period for complete mixing, and $I(0)$ is the average of the count rates for the D- and H-discs. The decay curves were fitted by a single-exponential function ($\Delta\rho(t)/\Delta\rho(0) = \exp(-k_{ex}t)$) to determine the exchange rate (k_{ex}).

For fluorescence experiments, n-(9-anthroyloxy)stearic acid (n-AS; n = 2, 6, or 12) was incorporated into nanodiscs or LUVs (DMPC:n-AS = 200:1). A series of n-AS species were purchased from Molecular Probes (Eugene, OR, for 2-AS and 12-AS) and Wako Pure Chemicals (Osaka, Japan, for 6-AS). The fluorophores of n-AS locate in the hydrocarbon region of the bilayers, depending on the position number n;[24,25] i.e., the larger n becomes, the deeper the fluorophores locate in the hydrophobic core of the bilayer. Experiments were performed with samples of 400 μM lipids in a quartz cuvette (10 mm thickness) at 27 °C. The mean fluorescence lifetime was measured on a Horiba NAES-550 nanosecond fluorometer (Kyoto). The steady-state fluorescence anisotropy was measured on a Hitachi F-4500 fluorescence spectrophotometer (Tokyo). These experimental procedures have been described in detail elsewhere.[26−28]

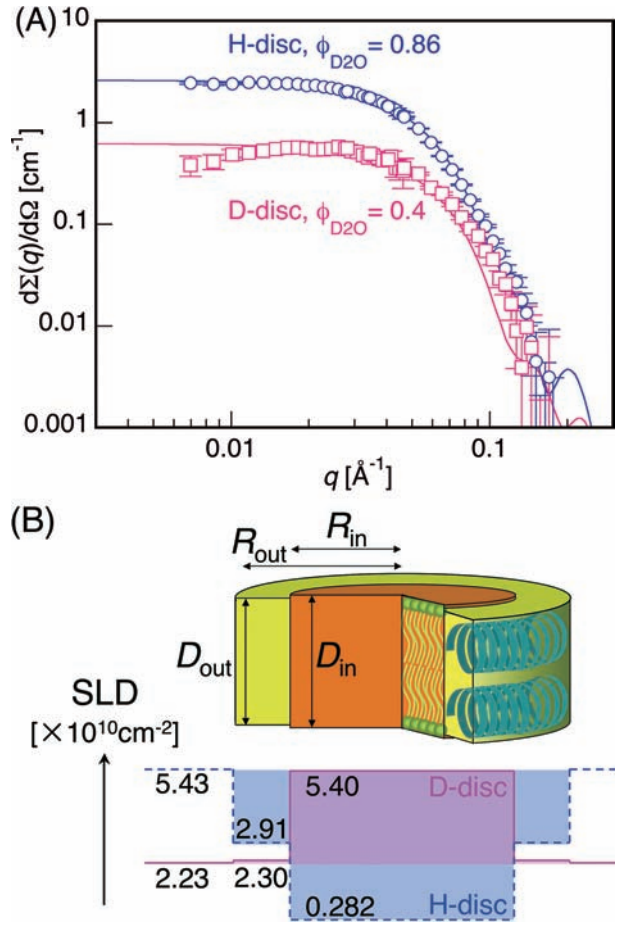

Figure 1. Structural evaluation of DMPC/apoA-I nanodiscs. (A) SANS profiles of a D-disc with $\phi_{D_2O} = 0.4$ and c_{PL} = 7.4 mM and an H-disc with $\phi_{D_2O} = 0.86$ and c_{PL} = 7.4 mM measured at 37.0 °C. Solid lines are fitting curves. (B) Structural model for SANS fitting. The rim of a lipid bilayer with a radius of R_{in} and thickness of D_{in} is surrounded by a protein ring with an outer radius of R_{out} and thickness of D_{out}. The scattering length density profiles of the D-disc ($\phi_{D_2O} = 0.4$) and H-disc ($\phi_{D_2O} = 0.86$) are represented by solid and dotted lines, respectively.

Theoretical Background. The scattering amplitude for a disc with a radius of R and a thickness of D is defined as[29]

$$A_{disc}(q,R,D,\theta) = V_{disc}\frac{2J_1(qR\sin\theta)}{qR\sin\theta}\frac{\sin(q(D/2)\cos\theta)}{q(D/2)\cos\theta} \qquad (1)$$

where $J_1(x)$ denotes the cylindrical Bessel function of first order, V_{disc} is the volume of the disc, i.e., $V_{disc} = \pi R^2 D$, and θ is the angle

(21) Segrest, J. P.; Jones, M. K.; Klon, A. E.; Sheldahl, C. J.; Hellinger, M.; De Loof, H.; Harvey, S. C. *J. Biol. Chem.* **1999**, *274*, 31755–31758.
(22) Handa, T.; Saito, H.; Tanaka, I.; Kakee, A.; Tanaka, K.; Miyajima, K. *Biochemistry* **1992**, *31*, 1415–1420.
(23) Okabe, S.; Nagao, M.; Karino, T.; Watanabe, S.; Adachi, T.; Shimizu, H.; Shibayama, M. *J. Appl. Crystallogr.* **2005**, *38*, 1035–1037.
(24) Abrams, F. S.; Chattopadhyay, A.; London, E. *Biochemistry* **1992**, *31*, 5322–5532.
(25) Waggoner, A. S.; Stryer, L. *Proc. Natl. Acad. Sci. U.S.A.* **1970**, *67*, 579–589.
(26) Kamo, T.; Nakano, M.; Kuroda, Y.; Handa, T. *J. Phys. Chem. B* **2006**, *110*, 24987–24992.
(27) Shintou, K.; Nakano, M.; Kamo, T.; Kuroda, Y.; Handa, T. *Biophys. J.* **2007**, *93*, 3900–3906.
(28) Fukuda, M.; Nakano, M.; Sriwongsitanont, S.; Ueno, M.; Kuroda, Y.; Handa, T. *J. Lipid Res.* **2007**, *48*, 882–889.
(29) Guinier, A.; Fournet, G. *Small-Angle Scattering of X-rays*; John Wiley: New York, 1955.

between the reference axis and the principal axis of the disc. By using eq 1, the scattering amplitude for a ring with outer radius R_{out}, inner radius R_{in}, and thickness D can be defined, i.e.

$$A_{ring}(q, R_{out}, R_{in}, D, \theta) = A_{disc}(q, R_{out}, D, \theta) - A_{disc}(q, R_{in}, D, \theta) \quad (2)$$

Then the scattering intensity for a discoidal lipid bilayer surrounded by proteins at the edge as a ring-shaped binder is derived as

$$I(q) = n \int_0^{\pi/2} \{(\rho_{disc} - \rho_s)A_{disc}(q, R_{in}, D_{in}, \theta) + (\rho_{ring} - \rho_s)A_{ring}(q, R_{out}, R_{in}, D_{out}, \theta)\}^2 \sin\theta \, d\theta \quad (3)$$

where ρ_{disc}, ρ_{ring}, and ρ_s are the scattering length densities (SLDs) of lipid, protein, and solvent, n denotes the number density of the particles, and D_{out} and D_{in} represent the thickness for the ring and the inner disc, respectively. $\int_0^{\pi/2}\sin\theta \, d\theta$ in eq 3 expresses the random orientation of the discs. The structure factor was assumed unity in eq 3 due to the very low concentration.

Results and Discussion

Structural Evaluation of Nanodiscs. Figure 1A shows the SANS profiles of these nanodiscs. On the basis of the above model with fixed values of the SLDs as shown in Figure 1B, two SANS profiles with different scattering contrasts were fitted simultaneously to estimate the size parameters. The estimated dimensions were R_{in} = 37 Å, D_{in} = 44 Å, R_{out} = 47 Å, and D_{out} = 42 Å. The thickness of the protein shell (10 Å) coincides with the diameter of α-helices. On the other hand, the height of the shell (42 Å) seems overestimated; according to the volume of two apoA-I molecules, D_{out} should be ca. 40% smaller than the estimated value. The large error is attributed to the fact that the size estimation for the protein layer relies only on the scattering of the H-disc, in which scattering from lipids nevertheless predominates over that from proteins. From the core volume and the specific volume of DMPC (0.985 mL/g),[30] the mean number of lipids in each nanodisc was calculated as 170 molecules/disc. This number accorded with that calculated from the absolute scattering intensity. The molecular area of DMPC was thereby calculated as 50 Å^2, which is much smaller than the molecular area in vesicles (65.7 Å^2)[31] and equal to the area of DMPC dihydrate,[32] corresponding to the smallest possible area.

To further investigate the static properties of DMPC/apoA-I nanodiscs and their differences compared to DMPC large unilamellar vesicles (LUVs), fluorescence lifetime and fluorescence anisotropy measurements were performed. Steady-state fluorescence anisotropy measurement is a well-established technique that detects the fluidity of membranes. As shown in Figure 2A, the steady-state fluorescence anisotropy of n-AS in nanodiscs decreased with an increase in n (i.e., deeper location of the fluorophore), which suggests increased fluidity at the bilayer center compared with the membrane interface. Obviously, each of the fluorescent probes showed much higher anisotropy in nanodiscs than in LUVs. This result denotes the higher acyl chain order in nanodiscs and suggests that DMPC molecules are more tightly packed into the protein ring. Figure 2B shows the mean fluorescence lifetime of 2-, 6-, and 12-AS for nanodiscs and LUVs. The fluorescence lifetime of fluorophores is known to be a measure of water penetration.[26,27,33] As expected, the lifetime increased with the position number n, as the fluorophores locate deeper into the hydrophobic core. The lifetime of 2-AS for nanodiscs was significantly longer than in LUVs, indicating a lower degree of water penetration into the membrane interface by nanodiscs, which supports the concept of increased acyl chain packing. 6-AS also showed a longer lifetime in nanodiscs. On the other hand, the lifetime of 12-AS was slightly shorter in nanodiscs than in LUVs, suggesting increased frequency of contact with water molecules at the acyl chain ends. This result appears to contradict with the increased acyl chain packing at a glance. However, this can be explained as a result of facile water penetration at the edge of the discs. That is, compared with fluorophores located in the central area of discs, fluorophores in the boundary lipid region are more exposed to water. We confirmed that the 12-AS-specific exposure to water was not due to the preferential location in boundary regions; fluorescence resonance energy transfer efficiencies[34,35] from tryptophan residues in apoA-I to 2-, 6-, and 12-AS were almost the same (see the Supporting Information), suggesting

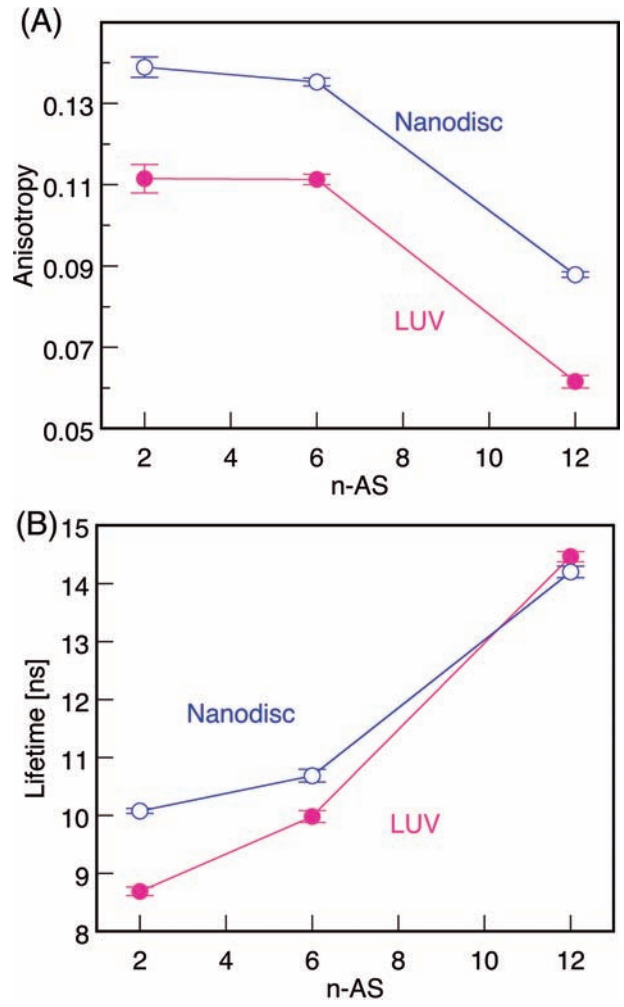

Figure 2. Steady-state anisotropy (A) and mean fluorescence lifetime (B) of n-AS (n = 2, 6, and 12) in DMPC LUVs and DMPC/apoA-I nanodiscs at 27.0 °C. Each point plotted against n represents the mean ± SD of three measurements.

(30) Nagle, J. F.; Wilkinson, D. A. *Biophys. J.* **1978**, *23*, 159–175.
(31) Lewis, B. A.; Engelman, D. M. *J. Mol. Biol.* **1983**, *166*, 211–217.
(32) Pearson, R. H.; Pascher, I. *Nature* **1979**, *281*, 499–501.
(33) Fiorini, R. M.; Valentino, M.; Glaser, M.; Gratton, E.; Curatola, G. *Biochim. Biophys. Acta* **1988**, *939*, 485–492.

no differential preference among these probes. Therefore, the higher contact frequency of 12-AS with water implies that water molecules penetrate between the protein belts and reach the acyl chain ends of the boundary lipids. Taken together, it is considered that lipids in nanodiscs experience an environment that is quite different from that of lipids in LUVs and is presumably entropically more unfavorable (but enthalpically favorable) due to the closer packing and hydrophobic hydration at the bilayer edge.

Energetic Consideration of Lipid Transfer from Nanodiscs. TR-SANS has been used to quantify the exchange dynamics in polymer micelles[36−38] and vesicles.[39] Previously, we performed TR-SANS measurements for DMPC LUVs and determined the half-life of the intervesicular lipid exchange to be ca. 440 min at 27 °C.[39] Here, we applied TR-SANS to nanodiscs to elucidate the dynamic properties of lipids in the particles. Unlike vesicles, outer and inner leaflets are indistinguishable for disclike particles, so that the decay of the contrast can be ascribed only to the interparticle exchange of DMPC. Figure 3A shows the contrast decays of nanodiscs. The decay curves at four different temperatures were reproduced well by a single-exponential function to provide the rate constant (k_{ex}). The decays were independent of the nanodisc concentration ($k_{ex} = 3.28 \times 10^{-2}$ and 3.78×10^{-2} min^{-1} at 13.3 and 20.0 mM, respectively, at 27.0 °C), which suggests that the lipid exchange is mediated not by a mechanism involving collisions between the discs, but by monomeric diffusion in an aqueous medium. Noteworthy, the decays were more than 20-fold faster than the theoretical decay with the exchange rate for LUVs (1.58×10^{-3} min^{-1}).[39] The Arrhenius plot for k_{ex} exhibited a good linear relationship (Figure 3B). Thermodynamic parameters at 37.0 °C were calculated according to the Eyring−Polanyi equation

$$k_{ex} = \frac{k_B T}{h} \exp\left(-\frac{\Delta H^{\ddagger} - T\Delta S^{\ddagger}}{RT}\right) \quad (4)$$

where k_B, h, and R are the Boltzmann, Planck, and gas constants, respectively. The obtained parameters were compared with those for LUVs.[39] From the k_{ex} values, the activation Gibbs free energies of transfer ($\Delta G^{\ddagger} = \Delta H^{\ddagger} - T\Delta S^{\ddagger}$) were calculated to be 91.8 and 101 kJ/mol at 37.0 °C for nanodiscs and LUVs, respectively (see Figure 4). Desorption of DMPC from LUVs involves a transition state that is both enthalpically ($\Delta H^{\ddagger} = 82.1$ kJ/mol) and entropically ($T\Delta S^{\ddagger} = -18.4$ kJ/mol) unfavorable.[39] On the other hand, $\Delta H^{\ddagger}$ and $T\Delta S^{\ddagger}$ for nanodiscs were 95.5 and 3.8 kJ/mol, respectively, suggesting that DMPC desorbs from nanodiscs via an enthalpically unfavorable but entropically favorable process. These distinct dynamic properties of lipids in nanodiscs, including a decreased (−9.2 kJ/mol) activation energy compared with that of LUVs, could be ascribed to the entropically more unstable state in nanodiscs as suggested by the static SANS and fluorescence measurements. That is, the lower entropy state derived from the closer lipid packing and hydrophobic hydration countervails the decremental entropy on the lipid desorption.

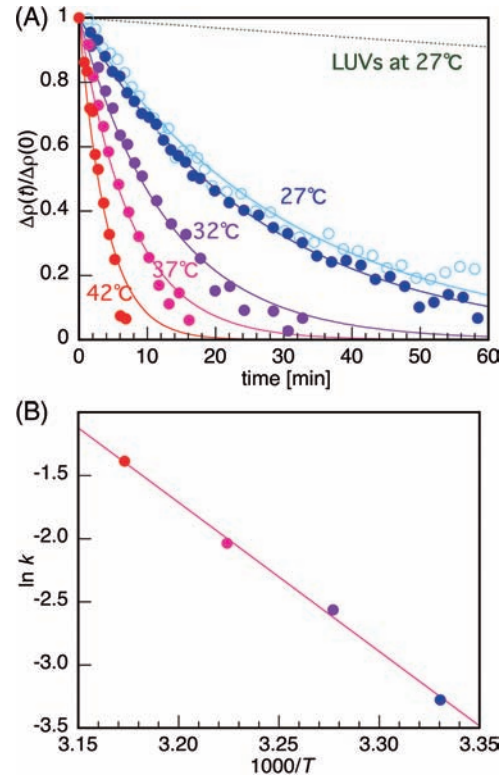

Figure 3. (A) Contrast decays after mixing of D- and H-discs of DMPC/apoA-I nanodiscs with $c_{PL} = 20.0$ mM (closed circles) and 13.3 mM (open circles) at four different temperatures. Solid lines are fitting curves with a single-exponential function. The dotted line is a theoretical single-exponential decay curve with an exchange rate corresponding to that of DMPC in LUVs at 27.0 °C ($k_{ex} = 1.58 \times 10^{-3}$ min^{-1}). (B) Arrhenius plot of the rate constant of interparticle exchange (k_{ex}).

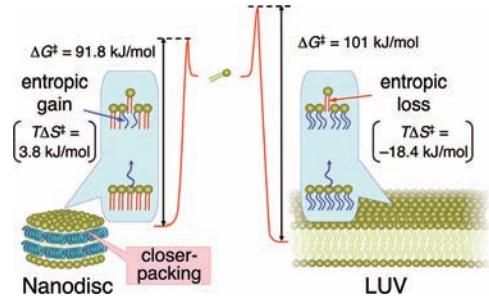

Figure 4. Schematic energy diagram of the transfer of phospholipids in nanodiscs and LUVs. Lipids in nanodiscs experience an environment that is entropically more unfavorable (but enthalpically favorable) due to the closer packing and hydrophobic hydration at the edge of the discs, as suggested by SANS and fluorescence measurements. These entropic constraints reduce an energy barrier of the transfer, resulting in the faster (more than 20-fold) transfer of DMPC.

In conclusion, the static and time-resolved SANS study in combination with fluorescence analysis clarified accelerated desorption of lipids in nanodiscs, which is connected with the static properties of bilayers altered by the envelopment with the proteins. These characteristics could relate to a drug release property of nanodiscs in pharmaceutical use and to cholesterol trafficking by discoidal high-density lipoproteins.

Acknowledgment. This work was part of joint research with the Institute for Solid State Physics, The University of Tokyo (Proposal Nos. 7616 and 8612). This study was supported by a

(34) Dergunov, A. D.; Dobretsov, G. E.; Visvikis, S.; Siest, G. *Chem. Phys. Lipids* **2001**, *113*, 67–82.
(35) Dobretsov, G. E.; Dergunov, A. D.; Taveirne, J.; Caster, H.; Vanloo, B.; Rosseneu, M. *Chem. Phys. Lipids* **1998**, *97*, 65–77.
(36) Willner, L.; Poppe, A.; Allgaier, J.; Monkenbusch, M.; Richter, D. *Europhys. Lett.* **2001**, *55*, 667–673.
(37) Lund, R.; Willner, L.; Richter, D.; Dormidontova, E. E. *Macromolecules* **2006**, *39*, 4566–4575.
(38) Lund, R.; Willner, L.; Stellbrink, J.; Lindner, P.; Richter, D. *Phys. Rev. Lett.* **2006**, *96*, 068302.
(39) Nakano, M.; Fukuda, M.; Kudo, T.; Endo, H.; Handa, T. *Phys. Rev. Lett.* **2007**, *98*, 238101.

Grant-in-Aid for Scientific Research from the Japanese Ministry of Education, Culture, Sports, Science and Technology (Nos. 17390011, 20050017, and 20790032) and the program for the Promotion of Fundamental Studies in Health Science of the National Institute of Biomedical Innovation (NIBIO).

Supporting Information Available: Fluorescence resonance energy transfer experiment with n-AS probes. This information is available free of charge via the Internet at http://pubs.acs.org.

JA9017013